Grafting Poly(*t*-butyl acrylate) to Poly(allylamine) by Inverse Microemulsion Radical Polymerization: From Comb-polymer to Amphiphilic Shell Crosslinked Polymer Nanocapsule

Debanjan Sarkar,[1] Jouliana M. El Khoury,[2] Stephanie T. Lopina,[1] Jun Hu[2]

[1]*Department of Chemical and Biomolecular Engineering, The University of Akron, Akron, Ohio 44325*
[2]*Department of Chemistry, The University of Akron, Akron, Ohio 44325*

Received 7 November 2005; accepted 12 February 2006
DOI 10.1002/app.25869
Published online in Wiley InterScience (www.interscience.wiley.com).

ABSTRACT: An interfacial grafting radical polymerization method for amphiphilic comb copolymer and shell crosslinked polymer nanocapsules was reported. Macropolyradicals on a water soluble long chain polyamine were generated with hydrogen peroxide in the water phase and subsequent grafting radical polymerization of a vinylic monomer at the water/oil interface proceeded at 65°C. In the presence of a crosslinker, the resulting graft copolymer formed a defined core-shell structure with hydrophilic aqueous core functionalized by the polyamine and a hydrophobic crosslinked polymer shell. The structure of the core-shell material was characterized by NMR, FTIR, DSC, TGA, SEM, TEM, and the mechanism of the graft polymerization is proposed. © 2007 Wiley Periodicals, Inc. J Appl Polym Sci 104: 1905–1911, 2007

Key words: amphiphilic copolymer; core shell polymer; inverse emulsion polymerization

INTRODUCTION

Recent advances in the synthesis of macromolecules allowed preparation of novel materials with nanoscopic architectures arising from self-assembly of the polymer domain structures.[1] Amphiphilic comb polymer is one of the complex macromolecular architectures that attracted much attention because of its unique supramolecular behaviors at the water–oil interface.[2,3] Several methods have been developed for comb polymers by copolymerization of long chain monomers (macromonomers)[4] or by condensation excess of reactive long chains with a multifunctional backbone polymer.[5] Although cationic,[6] anionic,[7] and condensation polymerization methods have been used,[5] controlled radical polymerizations, such as RAFT[8] and ATRP,[9] are most widely used. The amphiphilic nature of the comb polymer has not been exploited in the preparation of such materials by using radical polymerizations. We report a new method for producing amphiphilic comb polymers using inverse emulsion radical polymerization with a waterborne macroinitiator and oil-soluble monomer *t*-butyl acrylate (*t*-BA) (Scheme 1). In addition, the comb architecture of the resulting grafting copolymer was confirmed by self-assembling/nucleation and *in situ* crosslinking to form nanocapsules at the water–oil interface. We demonstrate that the microemulsion radical polymerization method is advantageous in terms of polymerization efficiency, product homogeneity, throughput, and cost of the initiating reagents.

Correspondence to: S. T. Lopina (lopina@uakron.edu) or J. Hu (jhu@uakron.edu).

Contract grant sponsor: National Science Foundation; contract grant number: DMR0210508.
Contract grant sponsor: National Institute of Health; contract grant number: DK61316-01.

© 2007 Wiley Periodicals, Inc.
WILEY InterScience® DISCOVER SOMETHING GREAT

EXPERIMENTAL

Materials

t-Butyl acrylate (*t*-BA, Aldrich, 98%) and ethylene diacrylate (ED, Acros, 70%) were washed with NaOH (MERCK, 97%) 5% aqueous solutions and dried over anhydrous $MgSO_4$ (Fischer, 99%) overnight and stored at −12°C prior to use. Poly(allylamine), (PAA, 20 wt % solution in water, M_w 17,000, Aldrich), H_2O_2, (30 wt % solution in water, Aldrich), toluene (Fischer, 99.9%), methylene chloride (Fischer 99.9%), and sorbitan monooleate (Span® 80, Aldrich) were used as received.

Synthesis of amphiphilic graft copolymer

A three-necked round-bottomed flask was equipped with a thermometer, a condenser, an argon inlet, and a magnetic stir bar. The flask was charged with

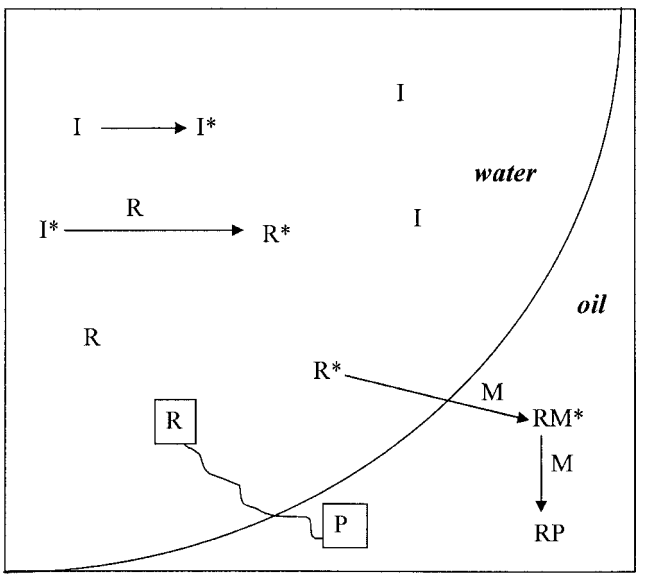

Scheme 1 Inverse emulsion polymerization: a route for an amphiphilic structure.

PAA (0.2 g in 5 mL of water), *t*-BA monomer (4.5 mL), ED (0.7 mL in 5 mL toluene), H_2O_2 (1.0 mL), and Span® 80 (0.17 g). The resulting mixture was sonicated (Fisher FS6) at room temperature for 30 min, resulting an inverse emulsion that was at least stable for 20 min when sitting at room temperature. The round-bottomed flask was placed in an oil bath and was heated at 65°C ± 2°C for 4 h under constant argon purge with uniform stirring with a magnetic stirrer (Corning). After the reaction, 50% v/v ethanol/water (30 mL) was added to the reaction mixture to precipitate the polymer. A yellowish sticky solid was obtained after removing the solvents and dried under vacuum at room temperature (0.7 g). ^{1}H NMR: δ 0.8–1.8 (polymer backbone, —CH_2—C—), 1.4 (*t*-butyl group, —C(CH_3)$_3$), 1.5 (acrylate chain, —CH_2—), 2.0 (acrylate chain, —C*H*— and amine, C—NH_2), 2.5 (methylene group in poly allylamine, —CH_2—N). ^{13}C NMR: δ 29.3 (*t*-butyl group, —C(CH_3)$_3$), 40.0 (methylene group in poly allylamine —CH_2—N), 37.0–39.0 (methyne carbons), 179.3 (carbonyl group).

Synthesis of core-shell material

A three-necked round-bottomed flask was equipped with a thermometer, a condenser, an argon inlet, and a magnetic stir bar. The flask was charged with PAA (0.2 g in 5 mL of water), *t*-BA monomer (4.5 mL), H_2O_2 (1.0 mL), and Span® 80 (0.17 g). The resulting mixture was sonicated (Fisher FS6) at room temperature for 30 min. The emulsion produced without ED was just as stable as the emulsion described earlier, and showed no phase separation during a period of about 20 min in room temperature. The reaction mixture was heated at 65°C ± 2°C for 4 h under constant argon purge with uniform stirring. The resulting milky suspension was diluted with water and stirred vigorously such that there was no aggregate in the mixture. The polymer was then collected by filtration and further dried under vacuum at room temperature to give a light yellow solid polymer. The product was then washed with methylene chloride to remove residual unreacted monomer and other impurities that were insoluble in water to produce the dry product (1.0 g). The final product was redispersed in water and stored at room temperature for a period of several weeks during the chemical, polymer structure, and morphological analyses, and through which time, no significant changes in the appearance of the material was observed.

Characterization of graft copolymer and core-shell polymer

The grafting density and efficiency of the copolymerization were analyzed according to the standard methods.[10,11] The copolymer product was washed with methylene chloride and water and was dried overnight under vacuum at room temperature to obtain the solid polymer particle. The grafting characteristics, reproducible within ±10%, were expressed by the following equations:

$$\text{Grafting percentage } (\%) = \frac{w_2 - w_1}{w_1} \times 100$$

$$\text{Grafting efficiency } (\%) = \frac{w_2 - w_1}{w_3} \times 100$$

$$\text{Grafting ratio } (\%) = \frac{w_1 - w_4}{w_1} \times 100$$

where, w_1, w_2, w_3, and w_4 are the weight of PAA, grafted-PAA, monomer, and nongrafted PAA, respectively (Table I).

Spectroscopic, thermal, and imaging characterization methods

NMR analysis was performed with a Varian Gemini 300 NMR spectrometer, and FTIR analysis was performed with a Nicolet NEXUS 870 FT spectrometer. For NMR characterizations, the PAA-*g*-poly(*t*-BA)

TABLE I
Grafting Characteristics of Amphiphilic Copolymer

Material	Grafting percentage (%)	Grafting efficiency (%)	Grafting ratio (%)
t-Butyl acrylate grafted poly(allyl amine)	239	24.5	88.5

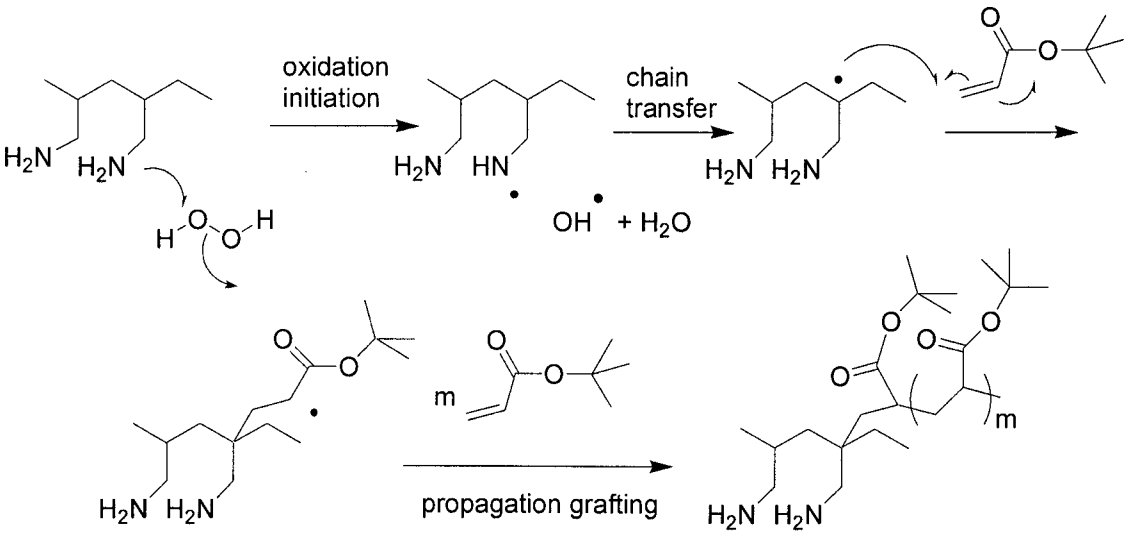

Scheme 2 Proposed mechanism of the polymerization.

comb polymer $CDCl_3$ was used a solvent and internal reference (7.20 ppm in ^1H NMR and 77.76 ppm for ^{13}C NMR). The shell crosslinked polymeric nanocapsules were insoluble in most of the NMR solvents. Differential scanning calorimetry studies of the solid polymer samples were performed with a DSC Q100V7.0 Build 244 (Universal V3. 7A TA) instrument at a scanning rate of 10°C/min. Thermogravimetric analysis (TGA) was performed with a TGA Q50V5.0 Build 164 (Universal V3. 7A TA) instrument. Scanning electron microscopy (SEM) studies were performed with a Hitachi S2150 instrument with an operating voltage of 15 kV. Transmission electron micrograph (TEM) was performed with a Jeol TEM (1200 EX II) at accelerating voltage of 120 kV.

RESULTS AND DISCUSSION

The new synthetic method is based on the generation of the initiating radical on a water soluble PAA backbone exclusively in the aqueous phase of an inverse microemulsion. Radical polymerization was thus confined at the water/oil interface with an oil-soluble *t*-BA. The radical chain propagated into the oil phase while the PAA backbone remained in the water phase (Scheme 1). The use of alkylamine and peroxides to initiate radical polymerization was established by Whitby and coworkers in 1950s.[12] However, most of the peroxides used in the initiation reactions are oil soluble. In addition, the exact mechanism for radical polymerizations using amine and peroxides is unclear. It was proposed that the oxidation of the amine group in the polymer generates the original nitrogen-centered radical species. Subsequent rearrangement of the nitrogen-centered radical to the carbon backbone of the polymer is thermodynamically favorable (Scheme 2). This process may be catalyzed by traces of metal ions such as Fe^{2+} in the reaction mixture, and may be inhibited by acids that

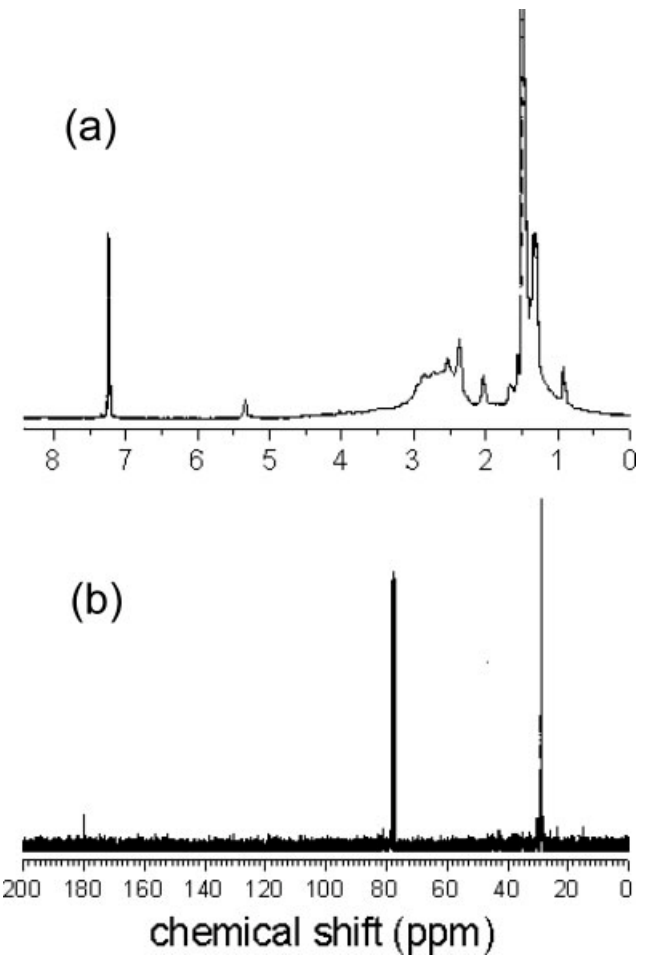

Figure 1 (a) ^1H NMR and (b) ^{13}C NMR of amphiphilic graft copolymer.

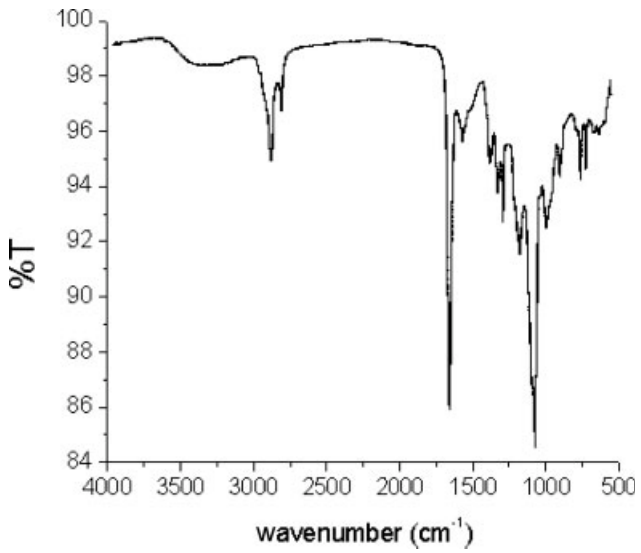

Figure 2 FTIR spectra of the polymer.

protonate the basic amine group.[13] To develop a waterborne radical macroinitiator, we examined the reactions between PAA and several oxidation agents including *t*-butyl hydrogen peroxide[14] and potassium persulfate.[15] We found that the combination of hydrogen peroxide (30% aqueous solution) and PAA initiated the radical polymerization smoothly in the water in oil microemulsion. The inverse microemulsion was produced by using Span® 80 (HLB = 4.3) as the main emulsifier. To obtain an inverse (W/O) emulsion, which is usually less stable than oil in water (O/W) emulsions, it is necessary to use a high concentration of emulsifiers having HLB value less than 7.[16] Electrostatic and/or steric factors are also important for the stability of the system.[16] In our case, we believe that the amphiphilic comb polymer also severed as surfactant during the polymerization with PAA as the aqueous soluble segment and poly (*t*-BA) as the hydrophobic segment. The unique comb polymer architecture of the PAA-*g*-poly(*t*-BA) provided additional stability to the microemulsion and ensured the radical chains only initiated on the water-soluble PAA backbone.

The formation of PAA-*g*-poly(*t*-BA) was evident from the solubility and increased mass of the solid products isolated from the reaction mixture. PAA readily dissolves in aqueous and highly polar solvents but not in toluene or other nonpolar solvents. The grafting polymerization product displayed typical amphiphilic copolymer characteristics, and dissolves readily in organic solvents such as CH_2Cl_2 and $CHCl_3$. Further studies of the polymer produce by ^1H and ^{13}C NMR spectroscopy showed the typical functionality of the proposed PAA-*g*-poly(*t*-BA) structure (Fig. 1).[17,18]

IR spectrum of the copolymer showed the strong band at 1728 cm^{-1}, the typical C=O stretching band for the carbonyl group of the acrylate ester, which indicated the presence of the poly *t*-BA segment in the copolymer. The broad band at 3200–3450 cm^{-1} is assigned to the *N*—H stretching and the small band at 1637 cm^{-1} is assigned to *N*—H waving. Both of these *N*—H peaks were present in the PAA spectrum, which indicated the PAA back bone remained in the copolymer product (Fig. 2). These results are consistent with the NMR data, indicating that the polymer product is a PAA-*g*-poly(*t*-BA) copolymer.

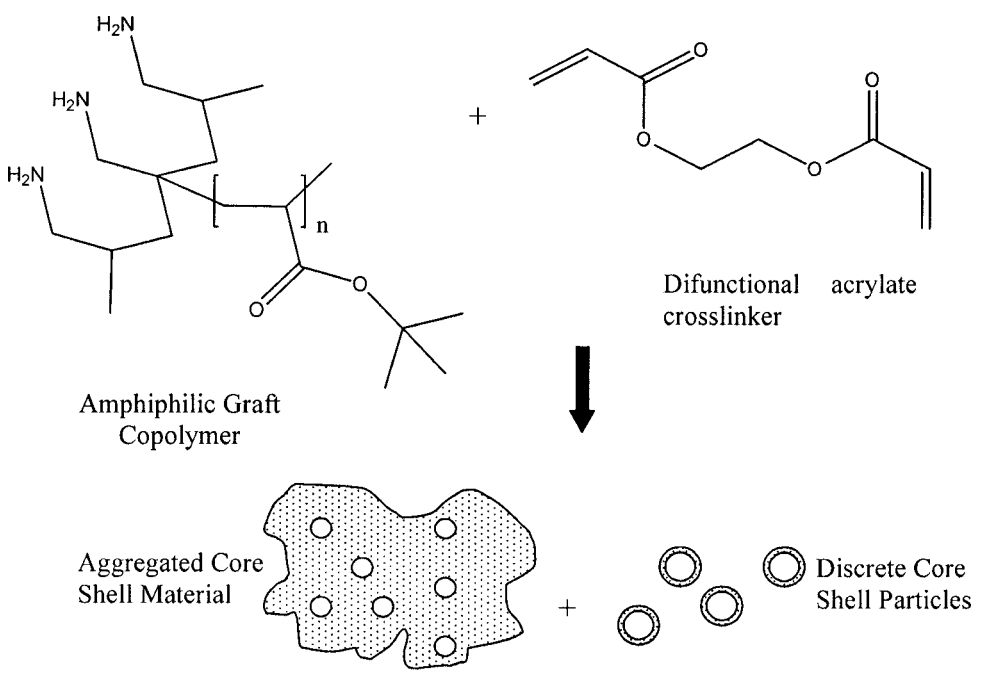

Scheme 3 Formation of shell crosslinked nanocapsules.

TABLE II
Solubility Characteristics of the Poly(allylamine)-*g*-poly(*t*-butyl acrylate) Copolymer Produced in the Inverse Microemulsion With *In Situ* Crosslinking

Solvent\Time	5 h	10 h	24 h	48 h
DMF	Insoluble	Swells	Swells	Almost soluble[a]
DMSO	Swells	Swells	Swells	Almost soluble[a]
Toluene	Swells	Swells	Almost Soluble[a]	Almost soluble[a]
Methylene chloride	Swells	Swells	Swells	Swells
Ethanol	Insoluble	Insoluble	Insoluble	Insoluble
Ethyl acetate	Insoluble	Insoluble	Insoluble	Insoluble
Water	Insoluble	Insoluble	Insoluble	Insoluble
Petroleum ether	Insoluble	Insoluble	Insoluble	Insoluble
Acetone	Insoluble	Insoluble	Insoluble	Insoluble
THF	Insoluble	Swells	Swells	Swells
Diethyl ether	Insoluble	Insoluble	Insoluble	Insoluble

[a] Solubility increases with increasing temperature.

It is well known that the core-shell morphology of a polymer produced in an emulsion is preferred only when the initiating radicals are formed at the water/oil interface and its diffusion to the interior of the emulsion is restricted.[12] We, thus, examined the formation of microcapsules by *in situ* crosslinking of the amphiphilic comb polymer with the dual objective of (1) to verify the interfacial polymerization mechanism for the comb polymer synthesis, and (2) to develop new methods of preparing shell crosslinked amphiphilic polymer nanocapsules, which are of a great deal interest in biomedical applications in our groups (Scheme 3).

The copolymer produced with the crosslinker showed limited solubility in organic solvents, which differed substantially to the corresponding uncrosslinked copolymer (Table II). Although PAA is soluble in water and insoluble in nonpolar organic solvents, the grafting copolymer showed substantial solubility in organic solvents such as toluene consistent with the amphiphilic nature of the copolymer product. The solubility of the crosslinker copolymer showed higher solubility in hydrophobic nonpolar solvents than the hydrophilic polar solvents. In nonpolar solvents, the polymer swells with time but remains almost unchanged for hydrophilic-polar solvents. This indicates that the outer shell of the polymer is more hydrophobic in nature and therefore is most likely to be the hydrophobic poly(*t*-BA).

The DSC thermogram of the PAA-*g*-poly(*t*-BA) copolymer produced in the inverse microemulsion with *in situ* crosslinking is shown in Figure 3. Two glass transitions (T_g's) were identified at about -1 and 55°C, indicating two possible polymer domains in the copolymer sample. In comparison, the thermogram of the parent PAA sample used in the synthesis displayed a single glass transition at ~ -6°C. Thus, the transition at ~ -1°C for the copolymer was assigned to the PAA segment of the copolymer. The transition at $\sim$ 55°C was assigned to the grafted poly(*t*-BA) segment because the T_g of poly(*t*-BA) is well known to be around 50°C.

TGA of the PAA-*g*-poly(*t*-BA) copolymer also displayed two decomposition stages at about 260 and 430°C, corresponding to the two main chemical components of the copolymer. In comparison, the PAA sam-

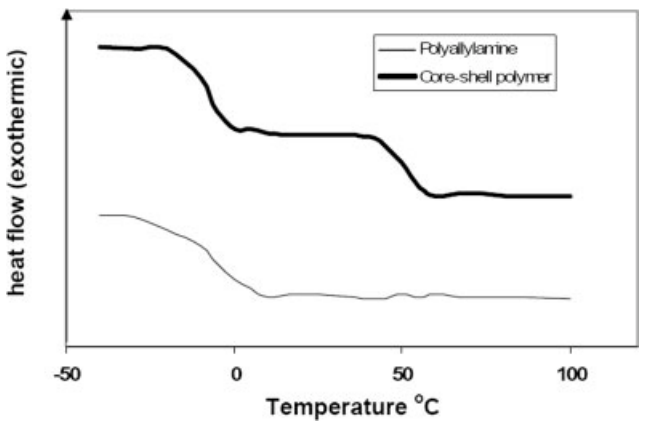

Figure 3 DSC thermograms of poly(allylamine) and poly (allylamine)-*g*-poly(*t*-butyl acrylate) copolymer.

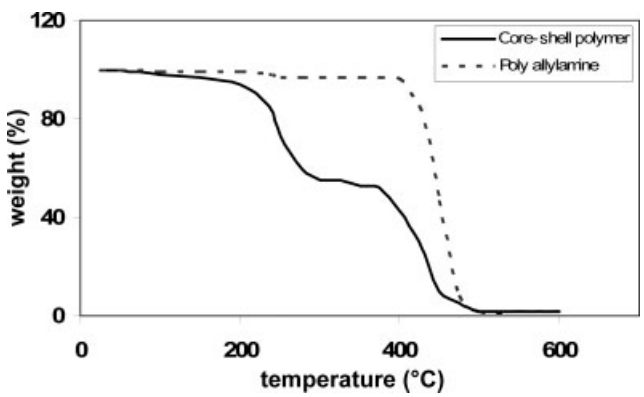

Figure 4 TGA thermograms of poly(allylamine) and poly (allylamine)-*g*-poly(*t*-butyl acrylate) copolymer.

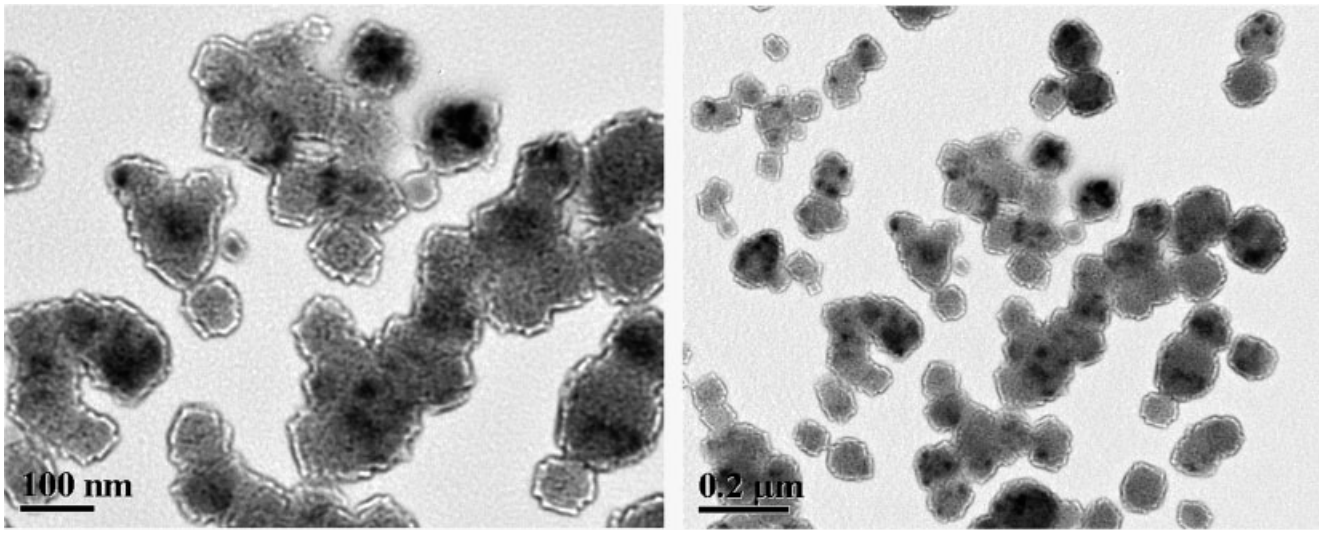

Figure 5 TEM images of the core shell material.

ple used in the synthesis showed a decomposition temperature at ~ 470°C. Thus, the first decomposition transition at about 260°C in the TGA was assigned to the decomposition of the poly(*t*-BA) segment of the copolymer where the *t*-butyl group can be recognized as the most labile functional group in the structure. The sec-

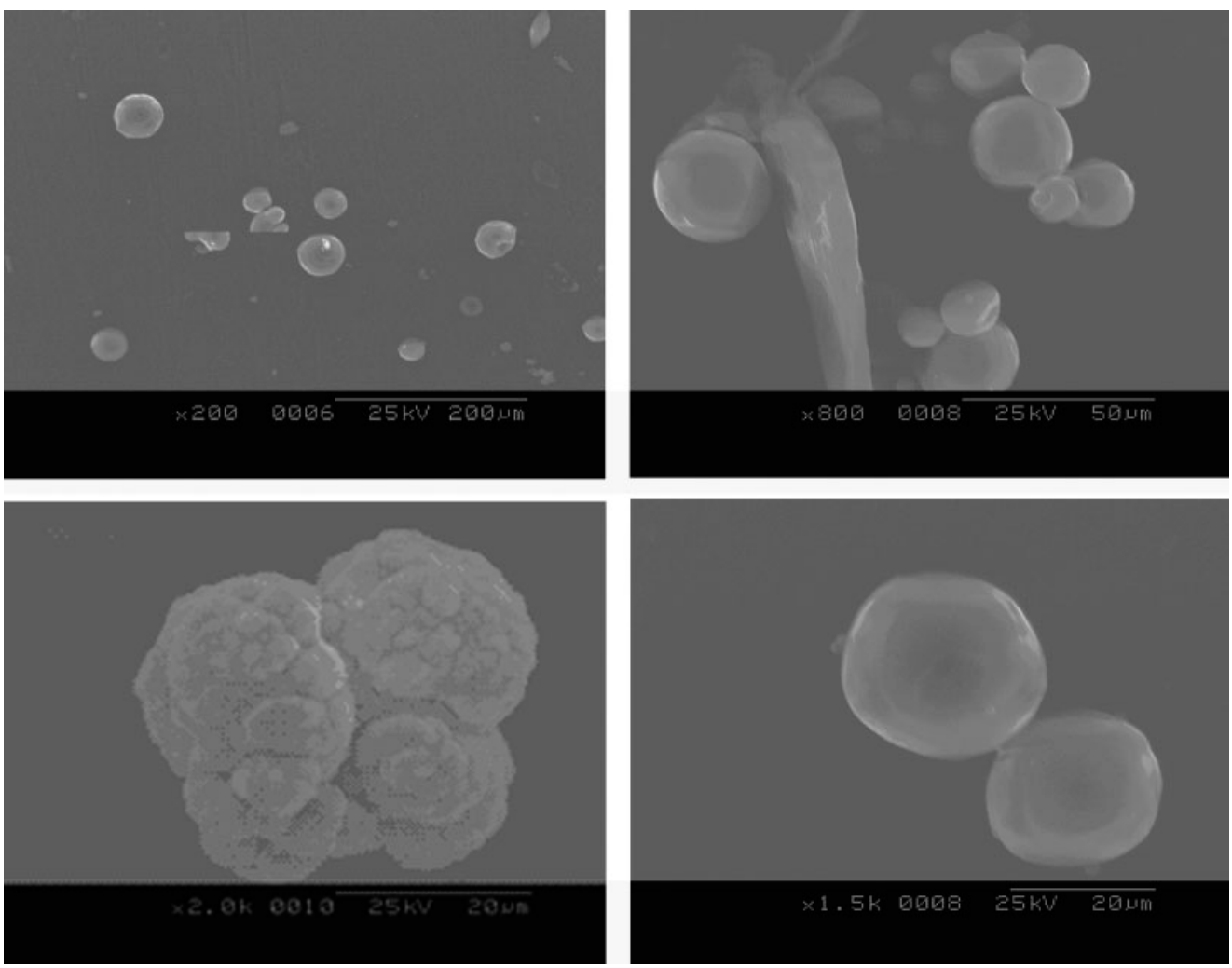

Figure 6 SEM micrographs core shell material: single particles and aggregated polymeric material.

ond transition in the TGA at about 430°C was assigned to the decomposition and related chemical reactions of the PAA. It can be estimated from the TGA analysis that the transition at 260°C corresponds to ~ 50% weight loss and the remaining 50% weight lost by 430°C. This indicated the poly(*t*-BA) segment is the major component of the copolymer (Fig. 4).

The above-mentioned spectroscopic and thermal characterizations provided strong experimental support for a PAA-*g*-poly(*t*-BA) comb copolymer architecture for the interfacial radical polymerization in the inverse microemulsion initiated by PAA and hydrogen peroxide. Examination of the copolymer produced by the interfacial grafting polymerization in the presence of a crosslinker with SEM and TEM imagining techniques revealed that the products displayed the typical spherical and shell morphology indicating the polymer product to be shell crosslinked copolymer capsules.

TEM analysis of the polymer sample provided conclusive evidence for the formation of nanosized polymer capsules in the microemulsion polymerization procedure with ED crosslinker. As shown in Figure 5, the TEM images of a dip-coated sample on a TEM grid from ~ 0.5 g/L suspension of the polymer nanocapsules in water displayed narrowly dispersed ~ 60 nm polymer nanocapsules. The nanocapsule shows a thin shell structure, which we believe to be the hydrophobic acrylic segment. The PAA interior is evident from the darker areas in the TEM images. The spherical morphology of the deformed nanocapsules in the TEM images were confirmed by SEM experiments of a similar polymer sample prepared with less surfactant and longer reaction time to increase the size of the polymer particles. The SEM images indicated that the product to be mostly discrete spheres of varied sizes with minor components of aggregates of irregular shapes (Fig. 6). From the images, it was also evident that the irregular aggregates increased with time and mechanical manipulations. The aggregation is thus attributed to physical crosslinking between the particles. The SEM and TEM results not only showed that the polymerization method is applicable for effective synthesis of the amphiphilic comb copolymers but also useful for the preparation of amphiphilic shell crosslinked polymer micro and nanocapsules.

The TEM and SEM results also showed that the interfacial grafting copolymerization method is highly efficient. The effectiveness of the method can be estimated by low reaction temperature and short reaction time. Quantitatively, the grafting percentage and grafting ratio for the typical polymerization reaction was shown in Table I. Most of the polyamine chains appeared to participate in the initiation process and to be grafted by the *t*-BA chains. The grafting efficiency, which indicates the amount of *t*-BA monomers resulted in the copolymer is consistent with a thin crosslinked shell structure in the sample shown in the TEM images (Fig. 5).

CONCLUSIONS

A new method for generating waterborne macroradical initiator at the water/oil interface is developed. Applying this new radical initiation system, we show that inverse emulsion polymerization can be exploited to synthesize amphiphilic comb polymers with the hydrophilic PAA backbone and hydrophobic side chains from radical polymerization of a hydrophobic monomer in the oil phase. The structure of the copolymer was confirmed by NMR, FTIR, DSC, and TGA analysis. The new material displayed typical amphiphilic comb polymer characteristics in the solubility studies. The mechanism of the microemulsion polymerization was investigated in the formation of shell crosslinked nanoscopic polymer capsules in the interfacial polymerization by TEM and SEM imaging. Amphiphilic polymer capsules of 50–1000 nm with well-defined nanostructures and surface functionalities can also be produced with the new interfacial polymerization method. We are currently in the process of using these polymer capsules for biosensing and drug delivery applications.

J. H. thanks the University of Akron Research Foundation for a startup grant and a faculty research fellowship.

References

1. Wooley, K. L. J Polym Sci Part A: Polym Chem 2000, 38, 1397.
2. Koh, A. Y. C.; Saunders, B. R. Chem Commun 2000, 2461.
3. Li, Z. C.; Jin, W.; Li, F. M. React Funct Polym 1999, 42, 21.
4. Xie, H. Q.; Liu, X. H.; Guo, J. S. J Appl Polym Sci 2003, 89, 2982.
5. Koutalas, G.; Iatrou, H.; Lohse, D. J.; Hadjichristidis, N. Macromolecules 2005, 38, 4996.
6. Kasuya, M. C.; Hatanaka, K. Macromolecules 1999, 32, 2131.
7. Ruckenstien, E.; Zhang, H. J Polym Sci Part A: Polym Chem 1999, 37, 105.
8. Liu, Q.; Zhang, P.; Lu, M. J Polym Sci Part A: Polym Chem 2005, 43, 2615.
9. Xia, J.; Zhang, X.; Matyjazewski, K. Macromolecules 1999, 32, 4482.
10. Athawale, V. D.; Lele, V. Carbohydr Polym 2000, 41, 407.
11. Chun, X. J Appl Polym Sci 1997, 64, 1733.
12. Whitby, G. S.; Wellman, N.; Floutz, V. W.; Stephens, H. L. Ind Eng Chem 1950, 42, 445.
13. Blackley, D. C. Emulsion Polymerization Theory and Practice; Wiley: New York, 1975.
14. Li, P.; Zhu, J.; Sunintaboon, P.; Harris, F. W. Langmuir 2002, 18, 8641.
15. Feng, X. D.; Guo, X. Q.; Qiu, K. Y. Die Makromol Chem 1988, 189, 77.
16. El-Asser, M. S.; Sudol, E. D. In Emulsion Polymerization and Emulsion Polymers; Lovell, P. A.; El-Aasser, M. S., Eds.; Wiley: New York, 1997; Chapter 2.
17. Kuo, P.-L.; Ghosh, S. K.; Liang, W.-J.; Hseih, Y.-T. J Polym Sci Part A: Polym Chem 2001, 39, 3018.
18. Hizal, G. Polymer 1996, 37, 541.